Preprints of the 21st IFAC World Congress (Virtual)
Berlin, Germany, July 12-17, 2020

Multivariable Feeding Control of Aluminum Reduction Process Using Individual Anode Current Measurement

Jing Shi, Yuchen Yao, Jie Bao, Maria Skyllas-Kazacos, Barry J. Welch

School of Chemical Engineering, University of New South Wales, Sydney, Australia
(*e-mail: j.bao@unsw.edu.au*)

Abstract: In the Hall-Héroult process, the alumina concentration and its distribution play an important role in determining the process efficiency, but it is difficult and costly to measure the concentration regularly. The recent advances in individual anode current measurement provide the possibilities to develop better control strategies and algorithms for alumina concentration. This paper presents a multivariable feeding control method, aiming to achieve a uniform distribution of alumina concentration, and hence improve cell operation. Also, the Extended Kalman Filter (EKF) is used to estimate the localized alumina concentration. The simulation results show that the proposed control strategy can significantly reduce the variations in alumina concentration compared to the traditional control method.

Keywords: Aluminum reduction process, individual anode current measurement, multivariable feed control, nonlinear state estimation

1. INTRODUCTION

The Hall-Héroult process has been dominating the aluminum production over a century (Grjotheim and Welch, 1980; Grjotheim and Kvande, 1993). The modern aluminum reduction cell uses molten cryolite (Na_3AlF_6) as the electrolyte to dissolve alumina (Al_2O_3). The main electrochemical reaction occurring at around 960 °C in the cryolite (usually called the 'bath') is represented by the equation:

$$2Al_2O_3(dissolved) + 3C(s) = 4Al(l) + 3CO_2(g) \qquad (1)$$

This reaction is driven by electrical current, normally referred to as the line current, having hundreds of kilo-amperes. This current is induced by parallel-connected carbon anodes, flowing through the bath and then collected by carbon cathode at the bottom of the cell. The voltage drop between anode and cathode is called the cell voltage. A schematic diagram of the aluminum reduction cell is shown in Fig. 1.

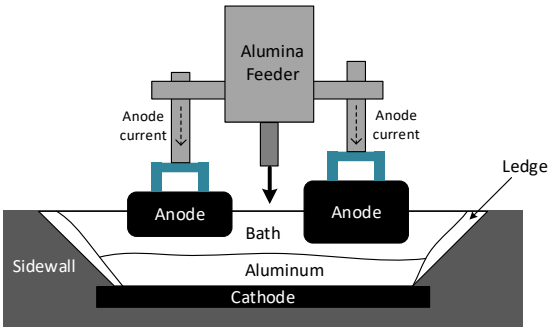

Fig. 1. Schematic diagram of an aluminum reduction cell

Alumina concentration is one of the most important process variables in the Hall-Héroult process because it is highly related to process safety and efficiency (Yao et al., 2017). In a modern aluminum reduction cell, alumina is fed by several point feeders located above the centerline of the cell, which can cause spatial variation of alumina concentration, especially for large cells. However, due to the harsh environment in the reduction cell, it is impractical to measure the alumina concentration regularly, and hence this limitation largely restricts the development of advanced control methods. The process variables that can be continuously measured are the line current and cell voltage, but they can only reflect the overall cell conditions. The traditional feeding control for the Hall-Héroult process is a logic-based method (Robilliard and Rolofs, 1989). The control action is determined according to the cell voltage. This method involves three predetermined feed rates and periods: base-feed (BF), overfeed (OF) and underfeed (UF). During the BF period, the alumina is fed into the cell at a nominal rate which is calculated from the theoretical consumption rate, whereas less alumina is fed during the UF period and more alumina is fed during the OF period. In practice, the alumina is fed into the cell in a discrete way, that is, a preset amount of alumina is dumped periodically through several feeders.

One of the most recent technological advancements for the Hall-Héroult process is the individual anode measurement (Cheung et al., 2013; Barnett, 1988; Evans, J. and Urata, N., 2012). It has been reported in a few papers in the literature (Yao et al, 2016, 2017) that the individual anode current measurement can help improve cell operation. Yao et al. (Yao et al, 2017; Yao and Bao, 2018) proposed several EKF-based algorithms to estimate localized cell information, including local alumina concentration, anode-cathode distance (ACD), bath flow, etc. These motivate the continued development of advanced multivariable feeding control methods. Although the terminology of multivariable control is not new in the aluminum smelting industry (Gran, 1980; McFadden et al., 2001, 2006; Moore and Urata, 2001; Moxnes et al., 2009), none of the publications contributed to individual feeding

control. Among these works, the model-based control is applied for the regulatory control of non-alumina electrolyte variables, including electrolyte temperature, aluminum fluoride concentration, liquidus temperature, superheat and electrolyte height. Nonlinear control (Kolås and Wasbø, 2010) is also introduced, but it is less attractive due to the difficulty of online implementation. In this paper, the LQR approach is used to control the alumina concentration. Different from the traditional method, the proposed controller is developed based on a discretized cell model and able to control the distribution of alumina concentration. The main advantage of this method is its simplicity, which makes online implementation promising. As a representative in modern control theory, LQR is attractive for the control of multiple inputs and multiple outputs (MIMO) systems. However, it fails to be robust to external disturbances and model uncertainties, leading to an offset. A common solution is to involve an integral action to eliminate the steady-state error (Bachir and Kamal, 2009, 2011; De Moura et al, 2019; Pang et al., 2011; Pannocchia, 2015). In addition, a nonlinear state estimator is developed based on the EKF technique to estimate alumina concentration. This paper is organized as follows. The process is briefly introduced in the next section, followed by the description of LQR and EKF. The control and estimation results are presented and compared with the traditional method. This paper concludes by discussing the advantages of the proposed control method and presenting some future work.

2.MATHEMATICAL MODEL OF ALUMINUM REDUCTION CELL

In this paper, the industrial aluminum reduction cell studied is shown in Fig. 2. This cell is operated at the line current of over 400 kiloamperes, consisting of 36 carbon anodes and 5 alumina feeders. The dynamics within the reduction cell are normally characterized by a set of mass balance equations (Yao et al., 2017), which are briefly discussed in this section.

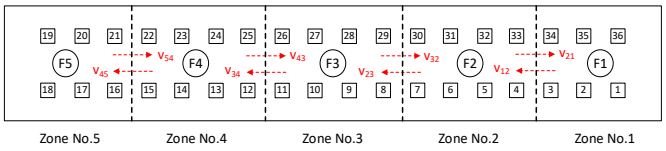

Fig. 2. Discretization of aluminum reduction cell according to feeder location

2.1 Mass Balance Model

For each zone shown in Fig. 2, there is one feeder which is responsible for supplying alumina powder. Therefore, the evolution of alumina concentration in one zone is mainly determined by the alumina consumption rate as well as its feeding rate. In addition, the local alumina concentration is correlated to bath flow pattern and velocity, which is assumed to be invariant in this work. Let us refer to Zone 2 as an example, then its discrete-time mass balance equations (Yao et al., 2017) at time k can be summarized:

$$C_{f,2}(k+1) = C_{f,2}(k) - k_1 C_{f,2}(k) + \frac{g_2(k) r}{m_2} \tag{2}$$

$$C_{s,2}(k+1) = C_{s,2}(k) - k_2 C_{s,2}(k) + \frac{g_2(k)(1-r)}{m_2} \tag{3}$$

$$\begin{aligned} C_{d,2}(k+1) = {} & C_{d,2}(k) + k_1 C_{f,2}(k) + k_2 C_{s,2}(k) \\ & - \frac{I_2(k) M \eta}{F z m_2} + \nu_{12} C_{d,1}(k) \\ & + \nu_{32} C_{d,3}(k) - \nu_{21} C_{d,2}(k) \\ & - \nu_{23} C_{d,2}(k) \end{aligned} \tag{4}$$

$$D_2(k+1) = D_2(k) - \delta_{a,2}(k) + \delta_{c,2}(k) + BM_2(k) \tag{5}$$

where $g_2(k)$ represents the mass of alumina fed by Feeder 2, and the alumina dissolves into the electrolytic bath with two different dissolution rates: a large portion (denoted by r) of alumina dissolves quickly with dissolution rate constant k_1, while the rest of the alumina dissolves in the same way but has dissolution rate constant k_2. Therefore, $C_{f,2}(k)$ and $C_{s,2}(k)$ are the mass concentration of fast-dissolved alumina and slow-dissolved alumina in Zone 2, respectively. $C_{d,2}(k)$ is the concentration of dissolved alumina in Zone 2, which is determined by several factors: 1) the amount of alumina dissolved; 2) the amount of alumina consumed which is governed by the Faraday's law of electrolysis; 3) the amount of alumina induced by bath flow from its neighboring zones. Here, $I_2(k)$ is the anode current flowing through Zone 2, M is the molar mass of alumina, η is the current efficiency, F is the Faraday's constant, and z is the number of electrons transferred. ν_{12} and ν_{23} represent the velocities of the bath flows from Zone 1 and Zone 3 to Zone 2. $D_2(k)$ is the average anode-cathode-distance (ACD) in Zone 2, which is determined by aluminum accumulation rate $\delta_{a,2}(k)$, anode consumption rate $\delta_{c,2}(k)$, and beam movement $BM_2(k)$.

For the purpose of alumina concentration control, this model can be rearranged in the form of a state-space model by selecting the state variable $X(k) \in \mathbb{R}^{15\times 1}$, input variable $U(k) \in \mathbb{R}^{5\times 1}$ and output variable $Y(k) \in \mathbb{R}^{5\times 1}$ as follows:

$$X(k) = \begin{bmatrix} X_1(k) \\ X_2(k) \\ X_3(k) \\ X_4(k) \\ X_5(k) \end{bmatrix}, U(k) = \begin{bmatrix} U_1(k) \\ U_2(k) \\ U_3(k) \\ U_4(k) \\ U_5(k) \end{bmatrix}, Y(k) = \begin{bmatrix} Y_1(k) \\ Y_2(k) \\ Y_3(k) \\ Y_4(k) \\ Y_5(k) \end{bmatrix} \tag{6}$$

where

$$X_i(k) = \begin{bmatrix} C_{f,i}(k) \\ C_{s,i}(k) \\ C_{d,i}(k) \end{bmatrix}, U_i(k) = g_i(k), Y_i(k) = C_{d,i}(k), \quad i = 1, 2, \cdots, 5 \tag{7}$$

2.2 Anode current and cell voltage

With the development in aluminum smelting industry, the anode current measurement is one of state-of-the-art technologies that has been used to monitor local cell conditions and hence improve cell performance (Yao et al., 2016). However, there is no explicit equation to describe the anode

current. Instead, it is correlated with cell voltage given by the following explicit empirical equation (Haupin, 1998):

$$V_{cell}(k) = f_v(I_i(k), D_i(k), C_{d,i}(k), \theta) \tag{8}$$

where f_v is a highly nonlinear function describing the cell voltage, and θ is a set of cell design parameters which can be regarded as constant.

3. CONTROL AND ESTIMATOR DESIGN

From the process model presented in Section 2, it can be seen that most of the nonlinearity of the process model lies in its output (voltage) equation (8) and the mass transfer dynamics (2)-(5) are fairly linear. Based on this observation, we propose a linear optimal control approach for the individual feeding control, integrated with a nonlinear state observer (an extended Kalman filter). This leads to an efficient control algorithm that can be effectively implemented in industrial alumimium reduction cells. The control inputs are individual alumina feeding rate, while the control outputs are alumina concentrations in different feeding zones.

3.1 Discrete-time state-space model

For simplification purpose, let us use x_k instead of $x(k)$ to represents state variable at time k, and this notation applies to other variables. If we consider the following deviation variables:

$$\Delta x_k = x_k - x_k^*, \Delta u_k = u_k - u_k^* \tag{9}$$

Then a linear model of the discretized cell can be obtained:

$$\begin{cases} \Delta X_{k+1} = A\Delta X_k + B\Delta U_k \\ \Delta Y_k = C\Delta X_k \end{cases} \tag{10}$$

Where, $\Delta X_{k+1} \in \mathbb{R}^{15\times 1}$ is the vector of deviation state variables, ΔU_k=$\mathbb{R}^{5\times 1}$ is the vector of deviation input variables, and $\Delta Y_k = \mathbb{R}^{5\times 1}$is the vector of output variables. $A \in \mathbb{R}^{15\times 15}$ is the system matrix, $B \in \mathbb{R}^{15\times 5}$ is the input matrix and $C \in \mathbb{R}^{5\times 15}$ is the output matrix. They are given by:

$$A = \begin{bmatrix} A_1 \\ A_2 \\ A_3 \\ A_4 \\ A_5 \end{bmatrix}, B = \begin{bmatrix} B_1 \\ B_2 \\ B_3 \\ B_4 \\ B_5 \end{bmatrix}, C = [C_1 \quad C_3 \quad C_3 \quad C_4 \quad C_5] \tag{11}$$

where $A_i \in \mathbb{R}^{3\times 15}$, $B_i \in \mathbb{R}^{3\times 5}$ and $C_i \in \mathbb{R}^{5\times 3}$ $(i = 1, 2, \ldots, 5)$ are referred to Zone i in the discretized cell. Similar to (2)-(5), let us use Zone 2 as an example:

$$A_2 = \left[\begin{array}{ccc|ccc|ccc|c} 0 & 0 & 0 & 1-k_1 & 0 & 0 & 0 & 0 & 0 & \\ 0 & 0 & 0 & 0 & 1-k_2 & 0 & 0 & 0 & 0 & \mathbf{0}_{3\times 6} \\ 0 & 0 & v_{12} & k_1 & k_2 & 1 & 0 & 0 & v_{23} & \end{array}\right]$$

$$B_2 = \left[\begin{array}{c|c|c} \mathbf{0}_{3\times 1} & \begin{matrix} r/m_2 \\ (1-r)/m_2 \\ 0 \end{matrix} & \mathbf{0}_{3\times 3} \end{array}\right], C_2 = \begin{bmatrix} \mathbf{0}_{1\times 3} \\ 0 \quad 0 \quad 1 \\ \mathbf{0}_{3\times 3} \end{bmatrix} \tag{12}$$

3.2 LQR control integrated with integral action

For a linear system (A, B, C), the LQR control is essentially a multivariable proportional regulator, which is determined by minimizing a cost function:

$$J = \int_0^\infty (x^T Q x + u^T R u) dt \tag{13}$$

where J is a scalar performance index. Q is the state weighting matrix, which is a positive semi-definite matrix and used to penalize the state variable, while R is the control weighting matrix, which is a positive definite matrix and used to penalize the control action. Both weighting matrices are square and symmetric. The control law (Douglas, 1972) is derived by solving an algebraic Riccati equation (ARE):

$$A^T P + PA - PBR^{-1}B^T P + Q = 0 \tag{14}$$

and the control law is:

$$u = -R^{-1}B^T P x \tag{15}$$

To eliminate the steady-state error in tracking control problem, the LQR control is normally implemented in its velocity form with integral action. This is realized by augmenting the error state, and the state vector in (9) can be extended by including Z_k:

$$\tilde{X}_k = \begin{bmatrix} \Delta X_k \\ Z_k \end{bmatrix}, \tilde{U}_k = \Delta U_k, Z_k = Y_k - r \tag{16}$$

where, r is the setpoint, and we have the following augmented state-space model:

$$\begin{cases} \tilde{X}_{k+1} = \tilde{A}\tilde{X}_{k+1} + \widetilde{B}\tilde{U}_k \\ Z_k = \tilde{C}\tilde{X}_k \end{cases} \tag{17}$$

where $\tilde{A} = \begin{bmatrix} A & 0 \\ CA & I \end{bmatrix}$, $\widetilde{B} = \begin{bmatrix} B \\ CB \end{bmatrix}$ and $\tilde{C} = [0 \quad I]$. Therefore, the alumina concentration control can be formulated as an infinite horizon optimal control problem:

$$\min_{\tilde{X}_k} J = \sum_{k=0}^{\infty} \tilde{X}_k^T \tilde{Q} \tilde{X}_k + U_k^T \widetilde{R} \tilde{U}_k \tag{18}$$

where $\tilde{Q}$ and $\widetilde{R}$ are weighting matrix with appropriate dimension.

The optimal control law is given by:

$$\tilde{U}_k = -\left(\widetilde{R} + \widetilde{B}^T S \widetilde{B}\right)^{-1} \widetilde{B}^T S \tilde{A} \tilde{X}_k \tag{19}$$

where S is the steady-state solution of the Riccati equation:

$$0 = \tilde{A}^T S \tilde{A} - S + \tilde{Q} - \tilde{A}^T S \widetilde{B}\left(\widetilde{R} + \widetilde{B}^T S \widetilde{B}\right)^{-1} \widetilde{B}^T S \tilde{A} \tag{20}$$

The control input which is implemented on the plant can be computed as:

$$U_k = U_{k-1} + \tilde{U}_k \tag{21}$$

3.3 EKF state estimator

Although the LQR approach can deal with multivariable control problem, it requires feedback from the state variables, which are mostly not measurable in many industrial applications. For the aluminum reduction cell, the state variables in (6) can be estimated by an Extended Kalman Filter (EKF) (Simon, 2006). Its procedure is briefly outlined in this section.

To simulate the real plant, the model in (2)-(6) can be written in the following form by including process noise ω_k and measurement noise ν_k.

$$\begin{cases} X(k) = f(X(k-1), U(k-1), \omega(k-1)) \\ V_{cell}(k) = h(X(k), U(k), I(k), \nu(k)) \end{cases} \tag{22}$$

where, $f(\cdot)$ is a vector of functions for mass balance equations, while $h(\cdot)$ is the equation of cell voltage. ω and ν are white noise with covariance W and V.

- Priori estimate of state variables and error covariance at k^{th} step

$$\hat{X}(k|k-1) = f(\hat{X}(k-1|k-1), U_2(k-1), 0) \tag{23}$$

$$P(k|k-1) = F(k-1)P(k-1|k-1)(F(k-1))^T + L(k-1)W(k-1)(L(k-1))^T \tag{24}$$

where, $F(k)$ and $L(k)$ are partial derivative matrices given by

$$F(k-1) = \left.\frac{\partial f}{\partial X}\right|_{\hat{X}(k-1|k-1)} \tag{25}$$

$$L(k-1) = \left.\frac{\partial f}{\partial \omega}\right|_{\hat{X}(k-1|k-1)} \tag{26}$$

- Posterior estimate of state variables and error covariance:

$$K(k) = P(k|k-1)\big(H(k)\big)^T \big(H(k)P(k|k-1)\big(H(k)\big)^T + M(k)V(k)\big(M(k)\big)^T\big)^{-1} \tag{27}$$

$$\hat{X}(k|k) = \hat{X}(k|k-1) + K(k)\big[V_m - h\big(\hat{X}(k|k-1), 0\big)\big] \tag{28}$$

$$P(k|k) = (I - K(k)H(k))\ P(k|k-1) \tag{29}$$

where, $H(k)$ and $M(k)$ are partial derivative matrices given by

$$H(k-1) = \left.\frac{\partial h}{\partial X}\right|_{\hat{X}(k|k-1)} \tag{30}$$

$$M(k-1) = \left.\frac{\partial h}{\partial \nu}\right|_{\hat{X}(k|k-1)} \tag{31}$$

Therefore, the overall control scheme includes discretized aluminum reduction cell, LQR-based controller and EKF estimator. This approach is illustrated in Fig. 3.

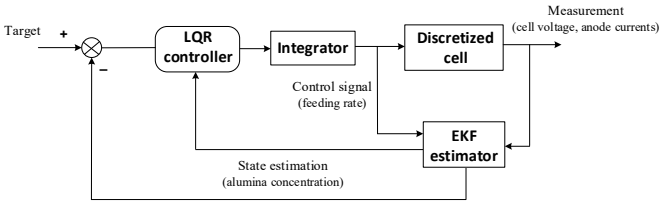

Fig. 3. Schematic diagram of alumina concentration control

4. SIMULATION RESULTS

In this section, the discretized aluminum reduction cell in Fig. 2 is simulated according to (2)-(6). The simulation results are presented by comparing the traditional feeding control method and the proposed LQR-based control method

4.1 Ideal operating conditions

The cell is firstly simulated and controlled by assuming that there is no model mismatch and external disturbance. The simulation is initialized with different alumina concentration and ACD in each zone: $C_{d0} = [3.3 \quad 2.8 \quad 2.9 \quad 3.2 \quad 2.6]$, $ACD_0 = [2.6 \quad 2.5 \quad 2.4 \quad 2.3 \quad 2.7]$. Using zones No.1 and No.3 as an example, the simulation is run for 20 hours and the results are shown from Fig. 4 to Fig. 7.

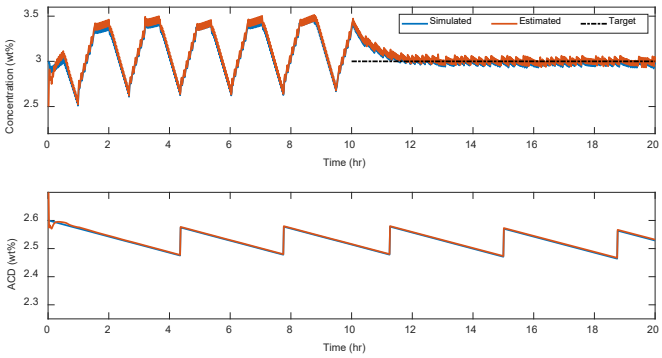

Fig. 4. Comparison of local alumina concentration in Zone 1 between the traditional and proposed methods

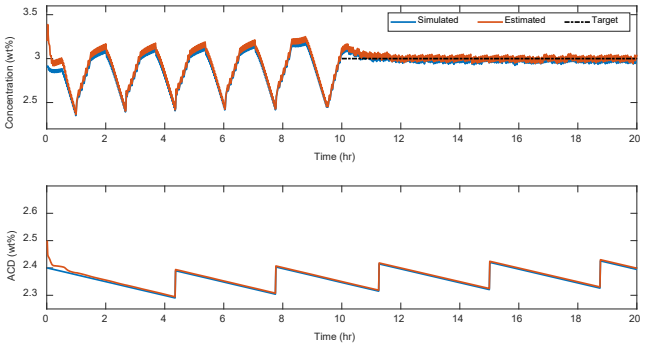

Fig. 5. Comparison of local alumina concentration in Zone 3 between the traditional and proposed methods

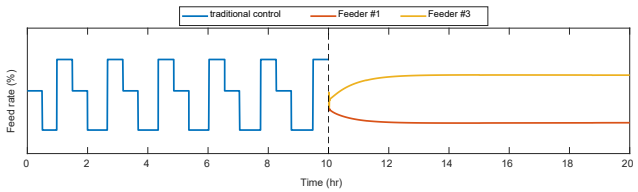

Fig. 6. Comparison of feed control rate between the traditional and proposed methods

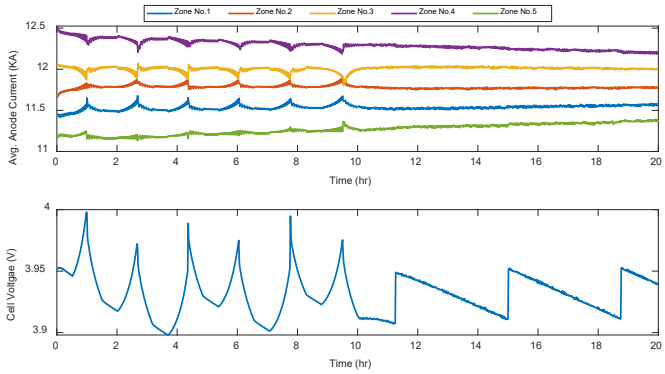

Fig. 7. Dynamics of anode currents and cell voltage

As shown in Fig. 4, the cell is initially controlled by the traditional method from $t = 0$ to 10 hr, and then the proposed controller takes over. The ACD is simulated to have a periodic lift-up to accommodate the effects from the metal accumulation and anode consumption. It is clear that the variation in alumina concentration is largely reduced both spatially and temporally when the proposed controller is applied, where the concentration is controlled at a set value. In the meantime, the variation in anode current and cell voltage is reduced shown in Fig. 7, which means a more stable and balanced cell.

4.2 Inaccurate dump weight

In practice, it is impossible to have a perfect model which can be used for control and estimator design. Therefore, the disturbance of inaccurate dump weight is introduced to test the robustness of the proposed control method. This is performed for both control methods and the comparisons are shown in Fig. 8 and Fig. 9.

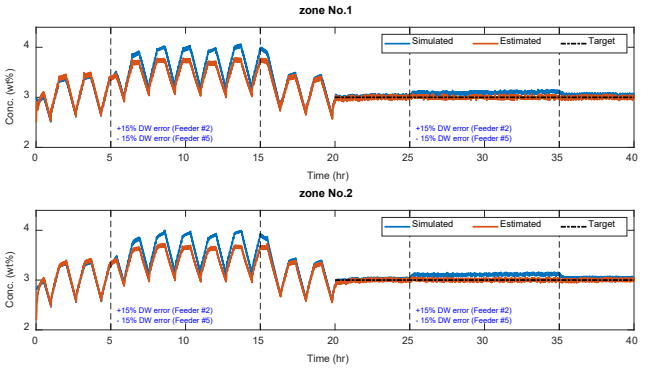

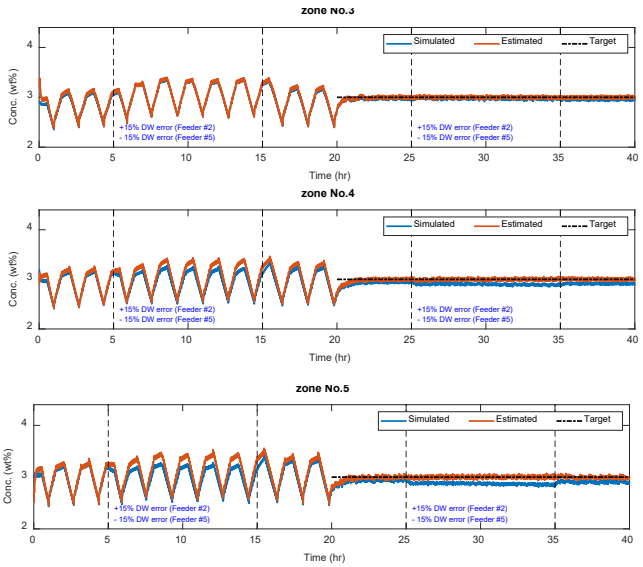

Fig. 8. Comparison of local alumina concentration between the traditional method and proposed method when dump weight is inaccurate

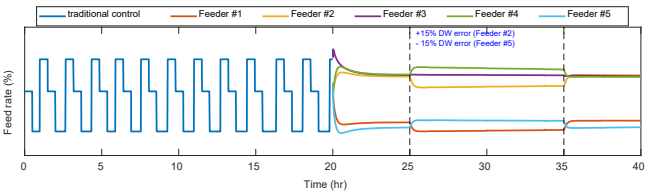

Fig. 9. Comparison of feed control rate between the traditional method and proposed method

Table 1. Mean Squared Error (MSE) between simulated and estimated concentration when a disturbance occurs

	MSE	
	Traditional Method	Proposed Method
Zone No.1	22.19	5.61
Zone No.2	24.30	7.44
Zone No.3	0.65	0.60
Zone No.4	7.20	5.72
Zone No.5	12.95	9.86
Mean	13.46	5.84

As shown in Fig. 8, inaccurate dump weight (DW) is simulated for Feeder 2 and Feeder 5, which is increased by 15% and decreased by 15% respectively. This is intentionally used to introduce local variations in the cell. As a comparison, this disturbance occurs in both control periods lasting for 10 hours, whereas it starts from $t = 5$ hr for conventional method and $t = 25$ hr for the proposed method. It is easy to see that the estimation cannot converge to the simulated value when the disturbance occurs, whereas the discrepancy between estimate and simulation is reduced by this new control method shown in Table.1. Although the estimation is inaccurate, the control

performance of the proposed method is still much better compared with the existing method. The main reason is that the proposed method is a multivariable controller and therefore can provide individual feeder action to control local alumina concentration. The integral action ensures that the estimated local alumina concentration, which is also the controlled variable, can be controlled at set-point without steady-state error.

5. CONCLUSIONS

This paper proposes a linear optimal control approach integrated with an extended Kalman filter for the nonlinear aluminum reduction process. This approach is motivated by the fact that most nonlinearity of the process model lies in its output (voltage) equation and the mass transfer dynamics are fairly linear. It has been shown that the proposed control method is effective in reducing the variation in alumina concentration. Compared with the traditional method, it is clear that the proposed method is superior in that it is more robust when dump weight is inaccurate. One of the advantages of the proposed control method is its simplicity, as only linear control is employed. This leads to efficient real-time control and implementation on the industrial plant. The further work of this paper will include the experiment studies by implementing the proposed control and estimation algorithms.

REFERENCES

Bachir, K. and Kamal, H. (2009). DSP-Based implementation of an LQR with integral action for a three-wire shunt active power filter, *IEEE Transactions on Industrial Electronics,* 56, 2821-2828.

Bachir, K. and Kamal, H. (2011). LQR with integral action applied to a wind energy conversion system based on double fed induction generator, *IEEE CCECE*, 717-722.

Barnett, W. (1988) Measuring current distribution in an aluminium reduction cell, U.S.Patent: 4786379.

Cheung, C.Y., Menictas, C., Bao, J., Skyllas-Kazacos, M., Welch, B.J. (2013) Characterization of individual anode current signals in aluminum reduction cells. *Industrial & Engineering Chemistry Research*. 52(28): 9632-9644.

De Moura, J.P., Rego, P.H.M. and Da Fonseca Neto, J.V. (2019). Online discrete-time LQR controller design with integral action for bulk Bucket Wheel Reclaimer operational processes via Action-Dependent Heuristic Dynamic Programming. *ISA transactions*, 90: 294-310.

Douglas, J.M. (1972) *Process Dynamics and Control: Control Systems Synthesis*, volume 2, 281-284 & 291-293. Prentice Hall Inc, Englewood Cliffs, New Jersey, USA.

Evans, J. and Urata, N. (2012). Wireless and non-contacting measurement of individual anode currents in Hall-Hérloult pots; experience and benefits. In *Proceedings of TMS Light Metals*, Orlando, FL. 939–942.

Gran, E. (1980) A multi-variable control in aluminum reduction cells. *Modeling Identification and Control*. 1(4): 247-258.

Grjotheim, K. and Welch, B.J. (1988). *Aluminium smelter technology--a pure and applied approach*. Aluminium-Verlag, Konigsallee.

Grjotheim, K. and Kvande, H. (eds.) (1993). *Introduction to aluminium electrolysis: understanding the Hall-Hérloult process*. Düsseldorf: Aluminium-Verlag.

Haupin, W. (1998). Interpreting the components of cell voltage. In *Proceedings of Light Metals*, San Antonio, Texas, 153-159.

Kolås, S. and Wasbø, S.O. (2010) A nonlinear model-based control strategy for the aluminium electrolysis process. In *Proceedings of Light Metals*, Seattle, WA, 825-829.

McFadden, F.J.S., Bearne, G.P., Austin, P.C. and Welch, B.J. (2001) Application of advanced process control to aluminium reduction cells–a review. In *Proceedings of Light Metals*, New Orleans, Louisiana, 1233-1242.

McFadden, F.J.S., Welch, B.J. and Austin, P.C. (2006) The multivariable model-based control of the non-alumina electrolyte variables in aluminium smelting cells. *JOM* 58(2): 42-47.

Moore, K.L. and Urata, N. (2001) Multivariable control of aluminum reduction cells. In *Proceedings of Light Metals*, New Orleans, Louisiana, 1243–1249.

Moxnes, B., Solheim, A., Liane, M., Svinsås, E. and Halkjelsvik, A. (2009). Improved cell operation by redistribution of the alumina feeding. In *Proceedings of Light Metals*, San Francisco, California, 461-466.

Pang, Z. H., Zheng, G. and Luo, C. H. (2011). Augmented State Estimation and LQR Control for a Ball and Beam System, *IEEE Conference on Industrial Electronics and Applications,* 1328-1332.

Pannocchia, G. (2015). Offset-free tracking MPC: A tutorial review and comparison of different formulations. In *Proceedings of 2015 European Control Conference (ECC)*, 527-532.

Pannocchia, G., and Rawlings, J. B. (2001). The velocity algorithm LQR: a survey. *Technical Report 2001-01, TWMCC*. Department of Chemical Engineering, University of Wisconsin-Madison, May 2001.

Potocnik, V., Arkhipov, A., Ahli, N., Alzarooni, A. (2017). Measurement of DC busbar currents in aluminium smelters. In *Proceedings of 35st International ICSOBA Conference*, Hamburg, Germany, 1113-1128.

Robilliard, K.R., and Rolofs, B. (1989). A demand feed strategy for aluminium electrolysis cells. In *Proceedings of Light Metals*, Indianapolis, Indiana, 747-751.

Simon, D. (2006). *Optimal state estimation*. John Wiley & Sons.

Yao, Y., and Bao, J. (2018). State and Parameter Estimation in Hall-Héroult Cells using Iterated Extended Kalman Filter. *IFAC-PapersOnLine*, 51(21), 36-41.

Yao, Y., Cheung, C.Y., Bao, J., Skyllas-Kazacos, M., Welch, B., and Akhmetov, S. (2016). Detection of local cell condition based on individual anode current measurements. In *Proceedings of TMS Light Metals*, Nashville, TN, 595-600.

Yao, Y., Cheung, C.Y., Bao J, Skyllas-Kazacos, M., Welch, B.J. and Akhmetov, S. (2017). Estimation of spatial alumina concentration in an aluminium reduction cell using a multilevel state observer. *AIChE,* 68(7), 2806-2818.